Int. J. Environ. Sci. Technol. (2014) 11:909–926
DOI 10.1007/s13762-013-0464-0

ORIGINAL PAPER

GIS-based frequency ratio and index of entropy models for landslide susceptibility assessment in the Caspian forest, northern Iran

A. Jaafari · A. Najafi · H. R. Pourghasemi · J. Rezaeian · A. Sattarian

Received: 2 July 2013 / Revised: 26 October 2013 / Accepted: 1 December 2013 / Published online: 10 January 2014

Abstract This study presents a landslide susceptibility assessment for the Caspian forest using frequency ratio and index of entropy models within geographical information system. First, the landslide locations were identified in the study area from interpretation of aerial photographs and multiple field surveys. 72 cases (70 %) out of 103 detected landslides were randomly selected for modeling, and the remaining 31 (30 %) cases were used for the model validation. The landslide-conditioning factors, including slope degree, slope aspect, altitude, lithology, rainfall, distance to faults, distance to streams, plan curvature, topographic wetness index, stream power index, sediment transport index, normalized difference vegetation index (NDVI), forest plant community, crown density, and timber volume, were extracted from the spatial database. Using these factors, landslide susceptibility and weights of each factor were analyzed by frequency ratio and index of entropy models. Results showed that the high and very high susceptibility classes cover nearly 50 % of the study area. For verification, the receiver operating characteristic (ROC) curves were drawn and the areas under the curve (AUC) calculated. The verification results revealed that the index of entropy model (AUC = 75.59 %) is slightly better in prediction than frequency ratio model (AUC = 72.68 %). The interpretation of the susceptibility map indicated that NDVI, altitude, and rainfall play major roles in landslide occurrence and distribution in the study area. The landslide susceptibility maps produced from this study could assist planners and engineers for reorganizing and planning of future road construction and timber harvesting operations.

Keywords Forest road construction · Mountainous terrain · Slope stability · Susceptibility modeling

A. Jaafari · A. Najafi (✉)
Department of Forestry, Faculty of Natural Resources, Tarbiat Modares University (TMU), P.O. Box: 64414-356, Noor, Mazandaran, Iran
e-mail: a.najafi@modares.ac.ir

H. R. Pourghasemi
Department of Watershed Management Engineering, Faculty of Natural Resources, Tarbiat Modares University (TMU), Noor, Iran

J. Rezaeian
Department of Industrial Engineering, Mazandaran University of Science and Technology, Babol, Iran

A. Sattarian
Department of Forestry, Faculty of Agriculture and Natural Resources, Gonbad Kavous University, Gonbad Kavous, Iran

Introduction

Landslides are the movement of a mass of rock, debris, or soil along a downward slope, due to gravitational pull (Das et al. 2012). The reasons for landslides are many, complex, convoluted, and every so often unknown (Yalcin et al. 2011). The significance of forestry activities such as road construction and timber harvesting in slope imbalance causing frequent occurrence of landslides is widely acknowledged (e.g., Larsen and Parks 1997). Timber harvesting in the north mountainous forest (Caspian region) of Iran moved on to steep terrain in the 1980s and early 1990s without a systematic approach for the identification of unstable terrain or down slope risks associated with road construction and timber harvesting. History has shown that roads with improper terrain stability assessment in this area can cause extensive and severe landslides (IPBO 2000).

High landslide frequency has resulted in large financial, social, and environmental costs in this area. This trend is not likely to decline soon; some estimates suggest that significant portions of forestland in the northern Iran are prone to mass wasting and the forestry activities that regularly happening on these lands have the potential to accelerate landslide rates and magnitudes (IPBO 2000). It is therefore critical to understand landslides and to find measures to mitigate subsequent losses to future landslides. Through scientific analyses, geoscientists and engineers can assess and predict landslide-prone areas, offering potential measures to decrease landslide damages (Oh and Pradhan 2011). Landslide susceptibility mapping (LSM) could be the basis for decision-making to help citizens, planners, and engineers to reduce the losses caused by current and future landslides by means of prevention, mitigation, and avoidance (Feizizadeh and Blaschke 2013). Various techniques and methods have been proposed and developed for the LSM purposes. They can be categorized into four groups depending on the modeling approach: statistical, analytic, deterministic, and heuristic techniques (Guzzetti et al. 1999). Each has its inherent advantages and limitations. For example, when study area is large, application of analytic methods is almost impossible (Pradhan 2013). The levels of landslide susceptibility determined by statistical methods are drastically affected by the accuracy of mapping of different conditioning factors and landslide inventory (Guzzetti et al. 1999). Das et al. (2012) address the issue of LSM along road corridors using Bayesian logistic regression models. They state that "heuristic approaches, in many instances, are biased as they depend on expert knowledge. Statistical methods, on the other hand, help to remove the bias of expert judgment and express the variability present in the datasets. Logistic regression is a robust and straightforward statistical method that is relatively easy to handle." Yilmaz (2009), in a comparative study, argues that "input process, calculations, and output process are very simple and can be readily understood in the frequency ratio model; however, logistic regression and neural networks require the conversion of data to ASCII or other formats. It is also very hard to process the large amount of data in the statistical package. On the other hand, all the three models have relatively similar accuracies." In general, these methods give rise to qualitative and quantitative maps of the landslide hazard areas, and the spatial results are appealing (Bui et al. 2012).

Independent of the modeling approach, the first step for assessing and managing of any landslide-prone area is to provide a landslide inventory map. The next step is the production of a LSM, which includes the spatial distribution of conditioning factors. This will allow landslide-prone areas to be delimited and indicate where landslides may likely occur in the future. The third step involves the creation of a landslide hazard map, which, in contrast to LSM, includes a temporal framework, with the probability of landslide occurrence within a specified period of time. The final step is the production of a landslide risk map, describing the expected annual cost of landslide damage throughout the affected area. Ultimately, all four maps are used to delimit and present zones of landslide susceptibility, hazard, and risk, respectively. A landslide zone is essentially a division of the land into areas and their classification according to degrees of actual or potential landslide hazard or susceptibility (Kamp et al. 2008).

The study was carried out in the Educational and Experimental Forest of Tarbiat Modares University (EEFTMU) in July–October 2012. The main objective of this study was to provide managers and foresters with a comprehensive assessment of landslide susceptibility in forestlands. For this purpose, we used frequency ratio and index of entropy models within a GIS environment. These models exploit information obtained from an inventory map, and a wide variety of conditioning factors to predict where landslides may occur in future. Furthermore, we provided a validation of the landslide susceptibility maps prepared for the study area. This study has practical implications for forest management and is novel; in that, it is the first replicated study in north mountainous forest of Iran to comprehensively assess the terrain stability for forestry activities.

Materials and methods

Study area

The study area is located in the EEFTMU, between the northern slopes of Albourz Mountains and southern shores of the Caspian Sea. The area lies between 36°29′10″N and 36°32′50″N latitude and 51°40′60″E and 51°48′20″E longitude, and covers an area about of 52 km^2 (Fig. 1). The area is a part of the Kojour watershed in the Caspian forest, with a rough topography, and a highest elevation of 2190 m a.s.l. The climate is humid and mild. The mean annual rainfall at the site is about 650 mm, falling mostly as rain and including a cover of snow in winters. The average summer and winter temperature are estimated to be 22.5 and 10 °C, respectively. The natural vegetation is a deciduous forest with dominant species of *Fagus orientalis* and *Carpinus betulus*. The geological, geomorphological, and hydrogeological environment of the area is favorable for landsliding. A number of landslides have occurred in the past; there are also numerous recorded instances of active landslides in this area. On the other hand, the forest managers had recently decided to construct new roads for timber harvesting operations. Hence, they need an assessment from landslide susceptibility in this area.

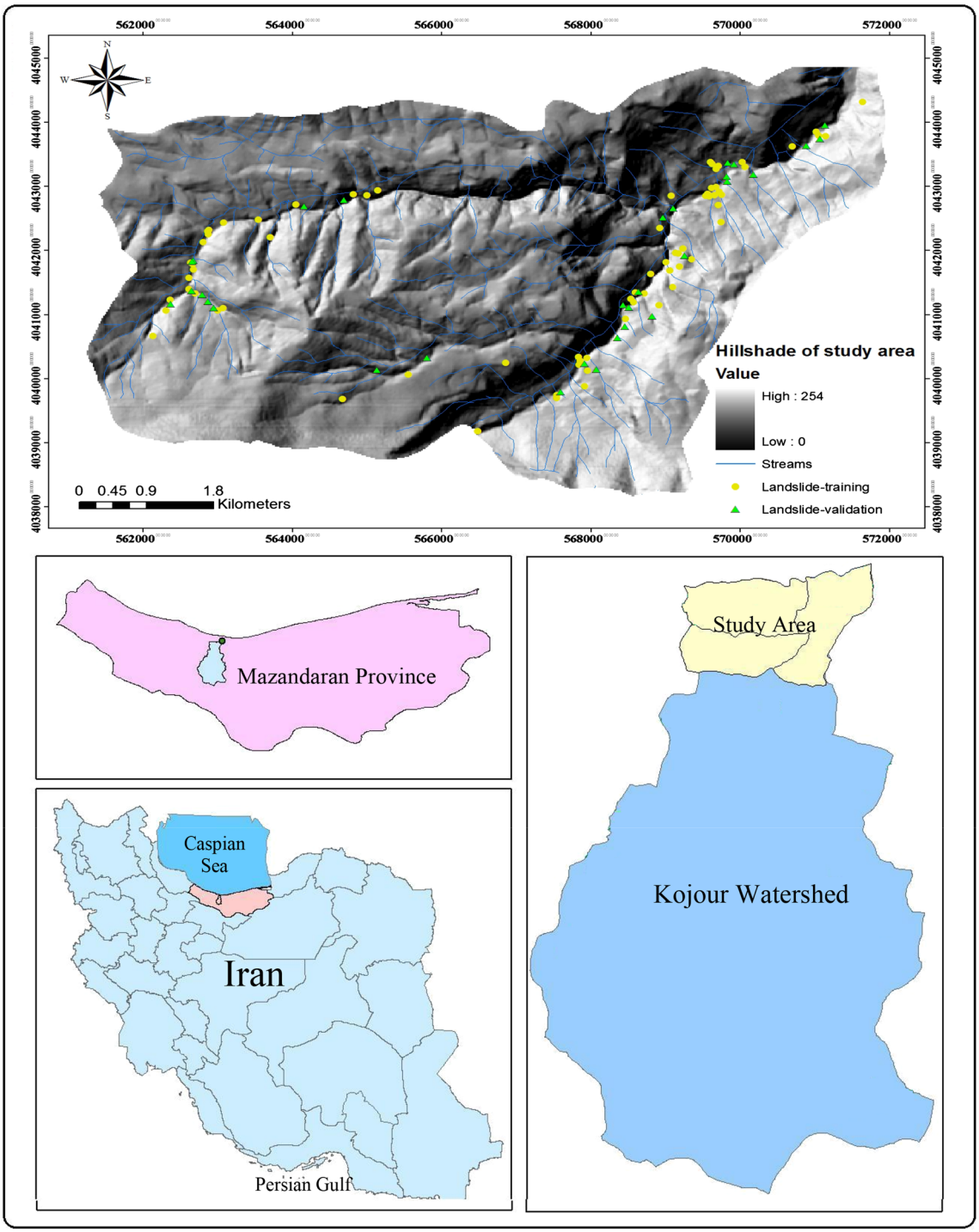

Fig. 1 Location of the study area with landslide location map

Data used

Landslide inventory map

Landslide inventory mapping is the systematic mapping of existing landslides in the study area using different techniques, such as field survey, aerial photograph, and satellite image interpretation, and literature search for historical landslide records (Ozdemir and Altural 2013). The landslide inventory map for our study area was compiled through aerial photographs interpretation and field-based inspection. In the aerial photographs, historical landslides could be observed as breaks in the forest canopy, bare soil, or geomorphological features, such as head- and side-

scarps, flow tracks, and soil deposits and debris deposits below a scar (Oh and Pradhan 2011). Given the abundant overstory and understory vegetation in the study forest, we also conducted multiple field surveys and observations to produce a more detailed and reliable landslide inventory map. A total of 103 landslides were detected in the study area (Fig. 1). 72 cases (70 %) out of 103 detected landslides were randomly selected for modeling, and the remaining 31 (30 %) cases were used for the model validation purposes (Mohammady et al. 2012; Pourghasemi et al. 2013).

Landslide-conditioning factors

The fundamental step for developing the predictive models of landslide occurrence is the recognition of the factors that are responsible for landsliding. The number of conditioning factors may range from only a few numbers to several (Mohammady et al. 2012; Pourghasemi et al. 2012b; Papathanassiou et al. 2012). The selection of these factors mainly depends on the availability of data for the study area and the relevance with respect to landslide occurrences (Papathanassiou et al. 2012). According to the Ayalew and Yamagishi (2005), in GIS-based studies, the selected factors should be operational, complete, non-uniform, measurable, and non-redundant. In this study, we considered a total of 15 landslide-conditioning factors. ArcGIS and SAGA GIS were employed to generate required conditioning factors. Slope degree, slope aspect, altitude, plan curvature, topographic wetness index (TWI), stream power index (SPI), and sediment transport index (STI) were extracted from a 20-m digital elevation model (DEM) (Fig. 2a–g). Given the physical relation between the landslide occurrence and slope gradient (Oh and Pradhan 2011; Pourghasemi et al. 2012b), substantial attention has been given for slope conditions in this study. The slope aspect is related to the general physiographic trend of the area. This factor strongly affects hydrological processes via evapo-transpiration and thus affects weathering processes and vegetation and root development. Altitude is also a significant landslide-conditioning factor because it is controlled by several geological and geomorphological processes (Dai et al. 2001). Plan curvature is described as the curvature of a contour line formed by intersecting a horizontal plane with the surface. The influence of plan curvature on the slope erosion processes is the convergence or divergence of water during downhill flow (Oh and Pradhan 2011). In the case of the plan curvature, positive curvature is an upwardly convex cell, zero curvature represent flat, and negative curvature is upwardly concave cell. The topography plays important role in controlling the spatial variation of hydrological conditions, such as soil moisture, groundwater flow, and slope stability (Yilmaz 2009). Secondary topographic attributes have been applied to describe spatial soil moisture patterns (Moore et al. 1991). One of these indices is the TWI developed by Beven and Kirkby (1979) within a runoff model. The TWI is the ratio between the specific catchment area and the slope (Moore et al. 1991):

$$\mathrm{TWI} = \ln\left(\frac{A_s}{\beta}\right) \tag{1}$$

where A_s is the specific catchment area (m^2/m), and β is slope angle in degrees. The TWI reflects the tendency of water to accumulate at any point in the catchment (in terms of a) and the tendency of gravitational forces to move that water down slope (Pourghasemi et al. 2012b). The other secondary derivative of the DEM is the SPI (Bagnold 1966). On the one hand, SPI is an indicator for erosive processes, as are caused by surface runoff. On the other hand, it is an indicator for the intermediate scale topographic position (ridge, slope, or valley bottom) (Vorpahl et al. 2012). The SPI is calculated from the following formula:

$$\mathrm{SPI} = A_s \times \tan\beta \tag{2}$$

where A_s is the specific catchment area (m^2/m), and β is slope angle in degrees. The next type of DEM-derived topographic data used in this study is STI. This index is equivalent to the length–slope factor in the Revised Universal Soil Loss Equation (Pourghasemi et al. 2012a) and often used to reflect the erosive power of overland flow. The STI is denoted mathematically by the Moore and Burch (1986) as below:

$$\mathrm{STI} = \left(\frac{A_s}{22.13}\right)^{0.6} \times \left(\frac{\sin\beta}{0.0896}\right)^{1.3} \tag{3}$$

where A_s is the specific catchment area (m^2/m), and β is slope angle in degrees. TWI, SPI, and STI can be easily produced as a function of standard terrain analysis within a SAGA GIS. The geological map prepared by Geological Survey of Iran (GSI) on 1:100,000 scale was used for the present study. The general geological setting of the area is shown in Fig. 3, and the lithological properties are summarized in Table 1 (Ghajar et al. 2012). The distance to streams was calculated using the topographic database (Fig. 4a). The distance to faults was calculated at 100-m intervals based on faults (Fig. 4b). The rainfall map was prepared using the mean annual precipitate data from the meteorological station for the study area over last 20 years (Fig. 5). In this study, a normalized difference vegetation index (NDVI) was also used as an environmental parameter for LSM (Fig. 6a). The NDVI is a measure of surface

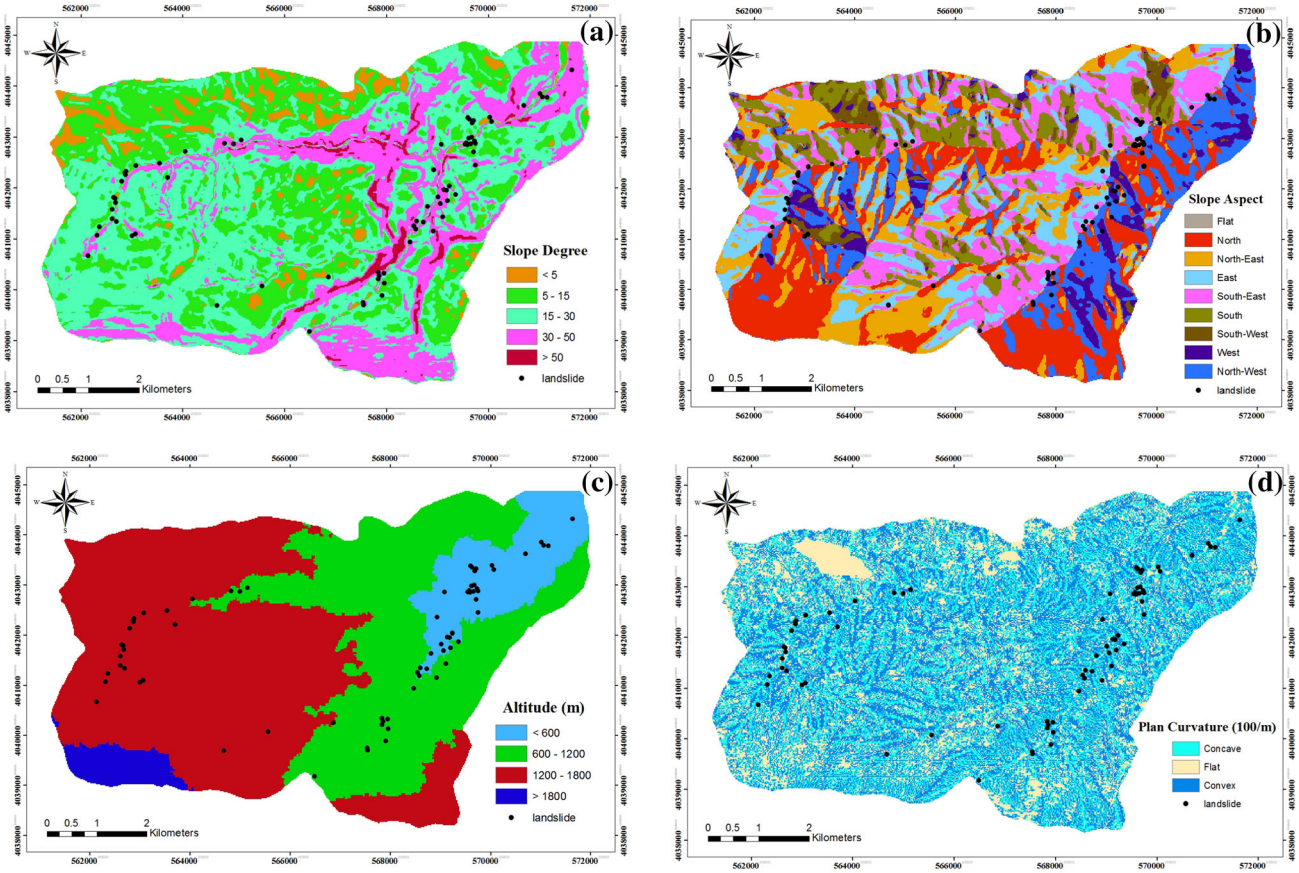

Fig. 2 Topographic parameter maps of the study area; **a** slope degree, **b** slope aspect, **c** altitude, **d** plan curvature; **e** topographic wetness index; **f** stream power index; **g** sediment transport index

reflectance and gives a quantitative estimate of vegetation growth and biomass (Hall et al. 1995). The NDVI is defined as follows:

$$\mathrm{NDVI} = \frac{(\mathrm{IR} - R)}{(\mathrm{IR} + R)} \tag{4}$$

where IR is the infrared portion of the electromagnetic spectrum, and R is the red portion of the electromagnetic spectrum. Low values of the NDVI (0.1 and below) indicate barren areas, sand, or snow. Moderate values (0.2–0.3) represent shrub and grasslands, whereas high values (0.6–0.8) correspond to temperate and tropical rainforests (Yilmaz and Keskin 2009). Forest canopy, timber volume, and plant community are also significant environmental parameters considered in this study (Fig. 6b–d). Given the important role of forest canopy in controlling many aspects of forest ecosystem dynamics (Sefidi et al. 2011), this index is incorporated as vital variables when modeling forest responses to the pressing issues (Didham and Fagan 2004). Timber volume (m^3/ha) has long been the most commonly used forestland attribute for providing information for the development of management strategies. Forest plant community is known to introduce some mechanical changes through soil reinforcement and slope loading (Abdi et al. 2010). The increase in soil strength due to root reinforcement has great potential to reduce the rate of landslide occurrence (Yalcin et al. 2011).

All the above-mentioned landslide-conditioning factors were stored in raster format with a cell size of 20 × 20 m and were overlaid with the landslide inventory map for the application of frequency ratio and index of entropy models.

Landslide susceptibility mapping (LSM)

Frequency ratio model

Mass movement and landslide-controlling factors are generally assumed to be similar to those observed in the past. If this assumption holds true, one can predict future slides occurring in a non-specified time span (Feizizadeh and Blaschke 2013). The frequency ratio model is based on the assumption that future landslides will occur at similar conditions to those in the past (Lee and Pradhan 2007). The frequency ratio is the ratio of the area where landslides

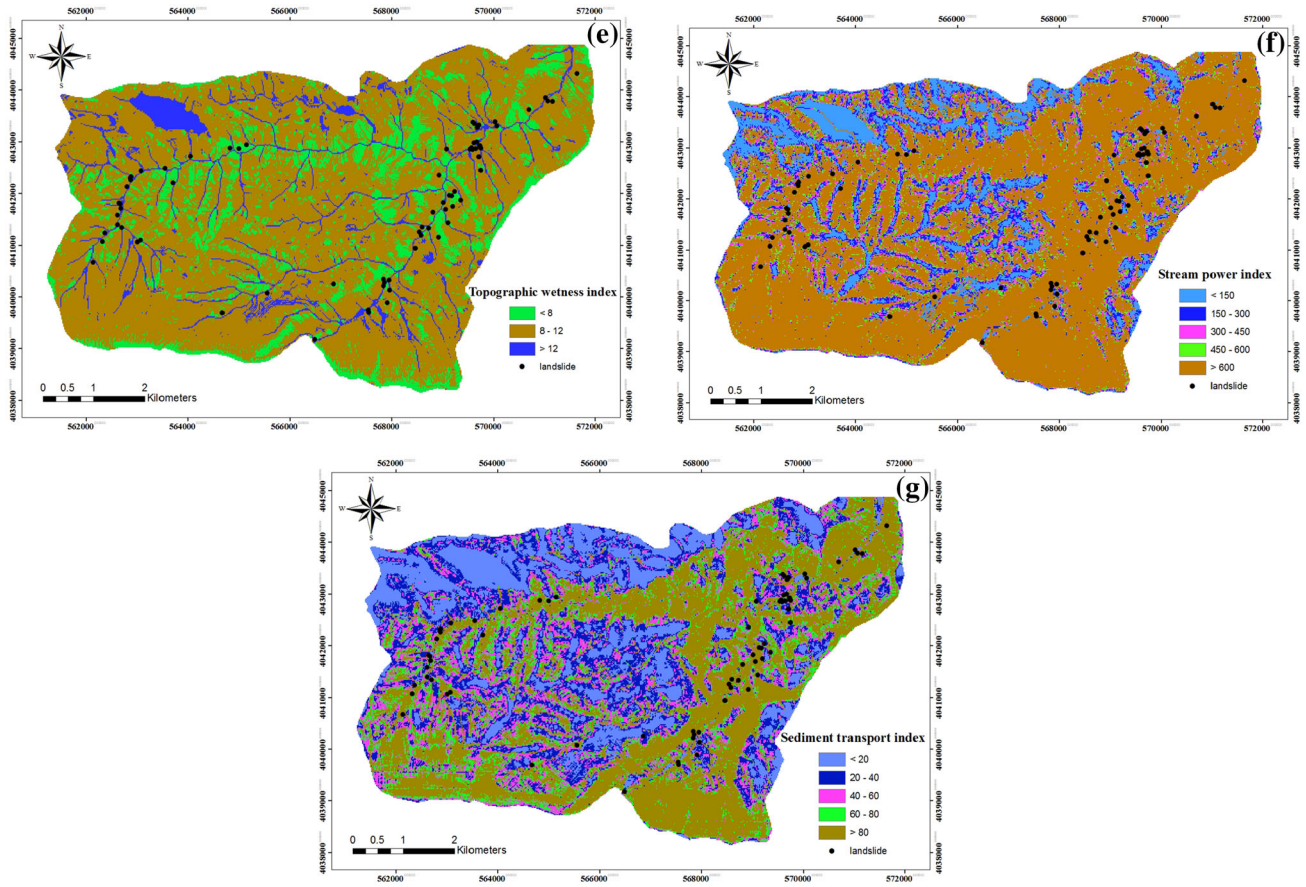

Fig. 2 continued

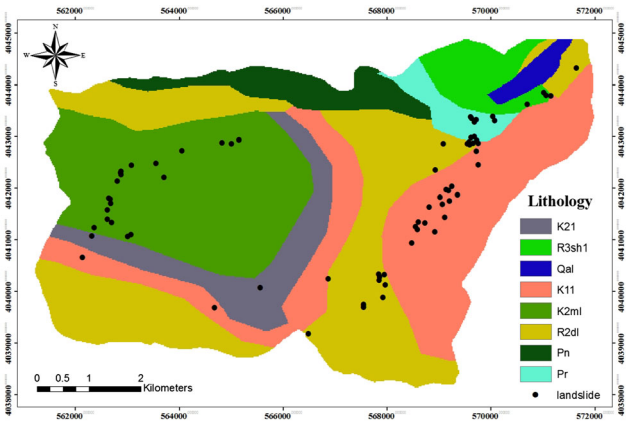

Fig. 3 The lithology map of the study area

have occurred to the total study area and is also the ratio of the landslide occurrence probabilities to the non-occurrence for a given attribute (Lee and Pradhan 2007). To calculate the frequency ratio, the area ratio of landslide occurrence to non-occurrence was calculated for each factor's type or range, after which an area ratio for the range or type of each factor to the total area was calculated. Therefore, the frequency ratio for each factor's class or type was calculated from its relationship with landslide events. The larger the ratio was, the stronger the relationship between landslide occurrence and the given factor's attribute (Yalcin et al. 2011). The landslide susceptibility index (LSI) was calculated by summation of each factor's ratio value using following equation:

$$\mathrm{LSI} = \sum \mathrm{FR} \tag{5}$$

where FR is rating of each factor's type or range. FR is expressed as follows:

$$\mathrm{FR} = \frac{\frac{N_{\mathrm{pix}}(SX_i)}{\sum_{i=1}^{m} SX_i}}{\frac{N_{\mathrm{pix}}(X_j)}{\sum_{j=1}^{n} N_{\mathrm{pix}}(X_j)}} \tag{6}$$

where $N_{\mathrm{pix}}(SX_i)$ is the number of pixels with landslides within class i of factor variable X, $N_{\mathrm{pix}}(X_j)$ is the number of pixels within factor variable X_j, m is the number of classes in the parameter variable X_i, and n is the number of factors in the study area (Regmi et al. 2013). The frequency ratio model can be simply implemented within a GIS environment, and the results are easy to understand (Yalcin et al. 2011; Mohammady et al. 2012; Ozdemir and Altural 2013).

Table 1 Types of geological formation of the study area (Ghajar et al. 2012)

Era (groups)	Geological age	Code	Lithology
Mesozoic	Cretaceous	K_1^l	Orbitolina limestone and calcareous shale
		K_2^l	Conglomerate in lower part, limestone, marly limestone, and sandy limestone
		K_2^{ml}	Limestone, marl, limy marl, and silty marl
	Triassic	$R_3^{sh,l}$	Shale, sandstone, and limestone
		R_2^{dl}	Thick-bedded to massive dolomitic limestone, dolomite, and limestone
Paleozoic	Permian	P_n	Cherty limestone, calcareous, and sandy shale
		P_r	Gray, thick-bedded to massive limestone and dolomite
Cenozoic	Quaternary	Q^{al}	Recent alluvium in river beds

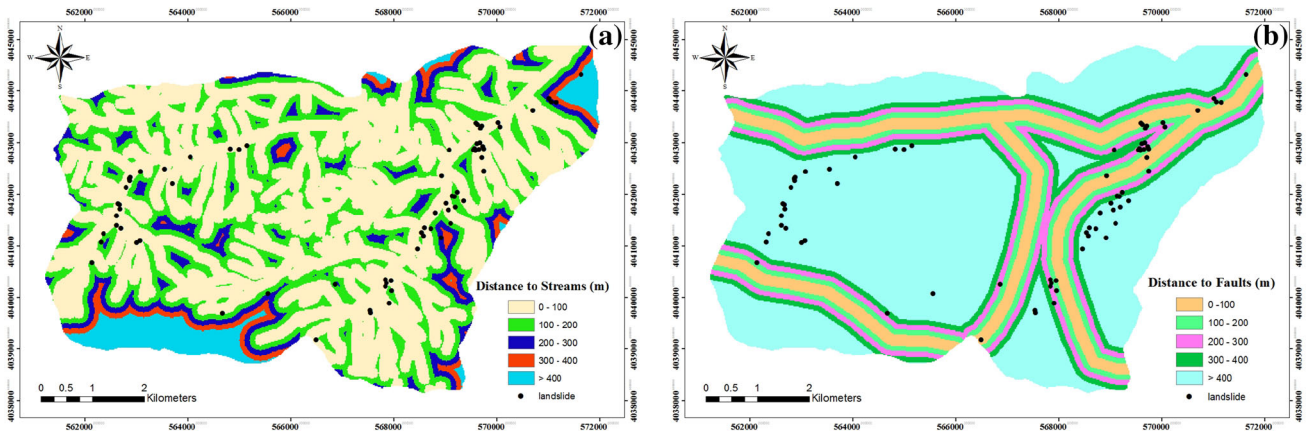

Fig. 4 Distance factors; **a** distance to streams, **b** distance to faults

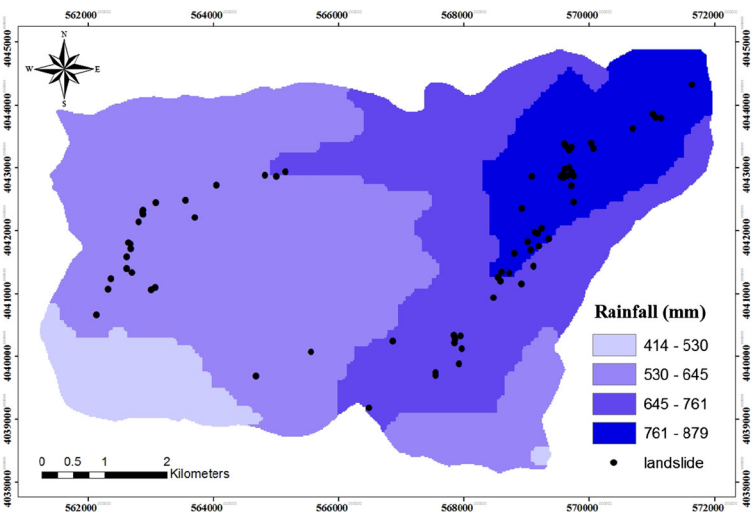

Fig. 5 The rainfall map of the study area

Index of entropy model

Another model used for LSM in this study is index of entropy model. The entropy indicates the extent of the instability, disorder, imbalance, and uncertainty of a system (Yufeng and Fengxiang 2009). The entropy of a landslide refers to the extent that various factors influence the development of a landslide (Pourghasemi et al. 2012b). Several important factors provide additional entropy into the index system. Therefore, the entropy value can be used to calculate objective weights of the index system. The equations used to calculate the information coefficient W_j

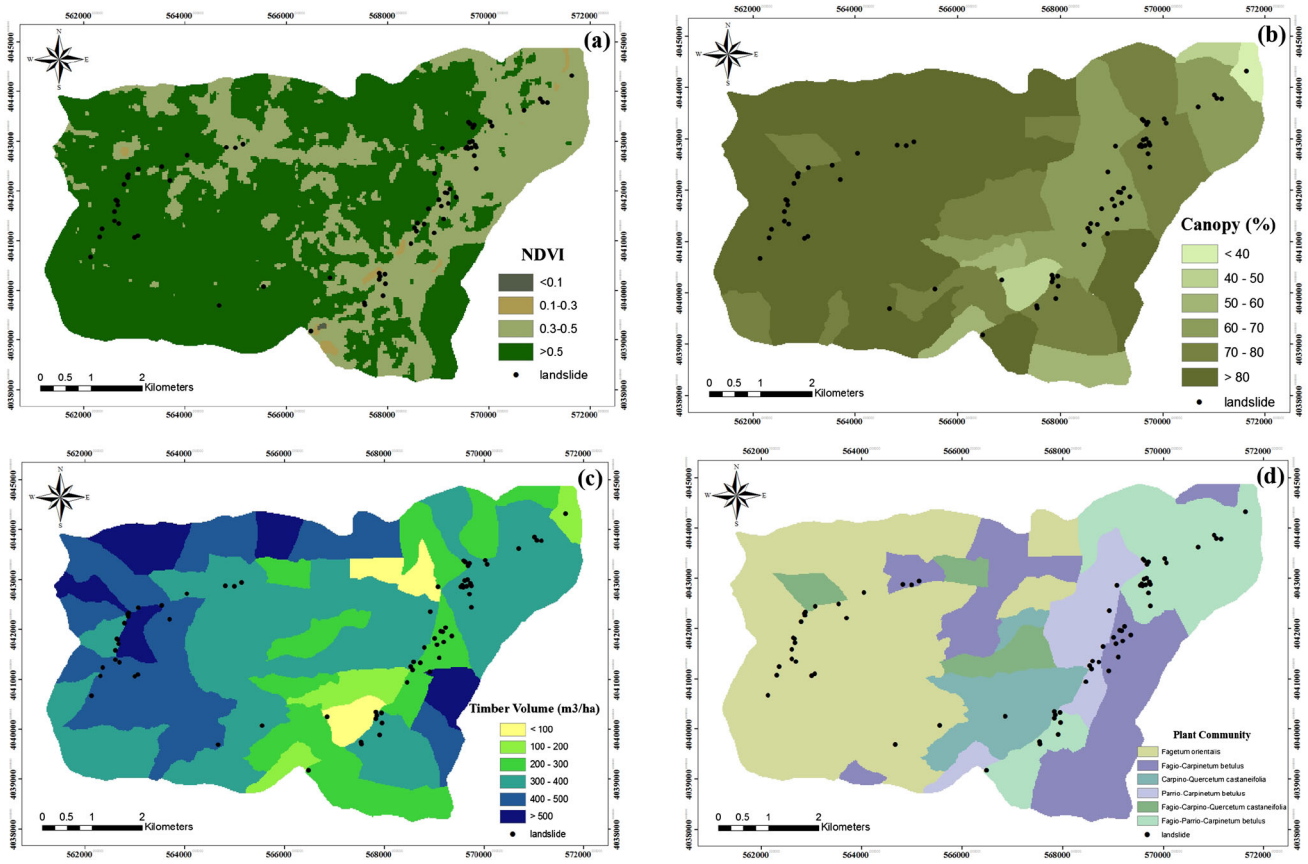

Fig. 6 Environmental parameter maps of the study area; **a** NDVI, **b** forest canopy, **c** timber volume, **d** plant community

representing the weight value for the parameter as a whole (Bednarik et al. 2010, 2012; Constantin et al. 2011) are the following:

$$P_{ij} = \frac{b}{a} \tag{7}$$

$$(P_{ij}) = \frac{P_{ij}}{\sum_{j=1}^{Sj} P_{ij}} \tag{8}$$

$$H_j = -\sum_{i=1}^{Sj} (P_{ij}) \log_2 (P_{ij}), \quad j = 1, \ldots, n \tag{9}$$

$$H_{j\max} = \log_2 S_j, \quad S_j \text{ is the number of classes} \tag{10}$$

$$I_j = \frac{H_{j\max} - H_j}{H_{j\max}}, \quad I = (0, 1), \quad j = 1, \ldots, n \tag{11}$$

$$W_j = I_j P_{ij} \tag{12}$$

where a and b are the domain and landslide percentages, respectively, (P_{ij}) is the probability density, H_j and $H_{j\max}$ represent entropy values, I_j is the information coefficient, and W_j represents the resultant weight value for the factor as a whole. The final landslide susceptibility map is prepared using the following equation:

$$Y_{\mathrm{IOE}} = \sum_{i=1}^{n} \frac{z}{m_i} \times C \times W_j \tag{13}$$

where Y_{IOE} is the sum of all the classes; i is the number of particular parametric map; z is the number of classes within parametric map with the greatest number of classes; m_i is the number of classes within particular parametric map; C is the value of the class after secondary classification; and W_j is the weight of a parameter (Bednarik et al. 2010; Devkota et al. 2013). The result of this summation represents the various levels of the landslide susceptibility (Constantin et al. 2011).

Results and discussion

Application of frequency ratio model

The result of the landslide susceptibility assessment based on the frequency ratio model shows that each class of the conditioning factors is characterized by a certain landslide occurrence density (Table 2). From table 2, it is seen that a slope angle in ranges of 30–50° and 30–50° shows 52.78

and 31.94 % of probability to landsliding with frequency ratio values of 1.25 and 1.50, respectively. The low probability of landslide occurrence is obtained in the areas having a steeper slope >50°. It is clear that the landslide occurrence increases by the increase in slope angle up to a certain extent, and then, it decreases. A similar pattern was also observed by Devkota et al. (2013). Generally, the shear stress is related to the slope. As the slope angle increases, the shear stress in the soil or other unconsolidated material generally increases. Gentle slopes are expected to have a low frequency of landslides because of the generally lower shear stresses are associated with low gradients (Mohammady et al. 2012). In the case of slope aspect, the value of frequency is higher for the areas facing the east, northwest, west, and southeast, and lower for flat and northeast. Previous studies (e.g., Fernandes et al. 2004; Ayalew and Yamagishi 2005) have also suggested that the high landslide density at specific slope aspects was associated with local conditions, such as the prevailing direction of winds and storms, fault orientation, rock structure, and even coastal erosion. However, some authors working in different areas have not noticed a significant relationship between landslides and slope aspect (e.g., Ayalew and Yamagishi 2004). For the altitude, landslide density is highest at the elevation ranging from 0 to 600 followed by 600–1,200 m. Meanwhile, altitude 1,200–1,800 m and >1,800 m show low frequency ratio, 0.59 and 0.00, respectively. Pachauri and Pant (1992) suggested that the higher elevation shows a greater susceptibility to sliding. However, in our study and based on the results reported by Ercanoglu and Gokceoglu (2002) and Pourghasemi et al. (2013), the higher topographic elevation is formed by the lithological units resistant to landslide and has a low frequency ratio. According to the results of the frequency ratio model, the more negative the curvature value, the higher is the probability of landslide occurrence. Relation between plan curvature and landslide probability shows that concave areas have a higher frequency ratio value (1.26) than convex areas (0.90), whereas flat areas have a low frequency ratio value of 0.83. The curvature area, in turn, will increase the moisture content of the soil, which will remain saturated, increase erosion, and decrease soil stability (Pourghasemi et al. 2013). The frequency ratio between landslide occurrence and TWI shows that the higher frequency ratio values are related to the class of >12 (2.49). Similarly, for SPI, the areas ranging on 450–600 and >600 have higher frequency ratio values (Table 2). In the case of the STI, landslide susceptibility is higher in areas where the STI ranges from 60 to 80 and >80. During the fieldwork, landslides were commonly observed on and close to relatively flat valley bottoms with a huge contributing area, where TWI, SPI, and STI expose higher values. Given that landslide initiation requires a contributing area of sufficient size combined with a minimum slope angle (Vorpahl et al. 2012), we expected low landslide susceptibility at low values of TWI, SPI, and STI. An analysis of the landslide distribution in relation to the geological formation types indicates that the P_r formation exhibits the highest frequency ratio (4.96), followed by the R_3^{sh1} formation (1.28). The other lithological units show different sensitivities to landslides (Table 2). Our results are in agreement with those of Gokceoglu et al. (2005), Lee and Pradhan (2007), and Ozdemir and Altural (2013), which have found that variations in landslide distribution are highly dependent on lithology type. For distance to streams, the frequency values show that when the distance increases, the probability of landslides decreases. The highest probability for landslide occurrence is within distances less than 100 m. Streams can adversely affect stability by eroding slopes or saturating the lower part of a material until the water level increases (Dai et al. 2001). However, landslides seem to occur most often at specific distances from the streams. For distance to faults, the landslide occurrence probability is high in areas where the distance is 100–200 and 200–300 m, whereas the probability decreases at a distance of less than 100 m or more than 300 m from a fault line. A similar trend was also reported by Ozdemir and Altural (2013). On the other hand, a different result was reported by Khanh (2009), who found that most landslides occur within a distance of 250–1,000 m. We attribute this difference to the local conditions, such as fault density, fault orientation, and rock structure. Investigation of rainfall indicates that for initiation of landslides in the study area, an intense rainfall is required. The frequency ratio in class of 762–879 mm is very high (3.19) than that of the other three classes. For NDVI values 0.3–0.5, the landslide frequency ratio was larger than 1, illustrating that relatively high vegetation coverage can easily lead to landslide occurrence. A positive correlation between landslide occurrence and NDVI was also reported by Yilmaz and Keskin (2009). The widely held view is that the vegetation coverage can protect slopes by reducing erosion, strengthening soil, and inhibiting landslides, which increase general slope stability (Bell 1998; Abdi et al. 2010). However, huge hardwood trees in the study area exposed to wind may transmit the forces into the slope and cause slope failure by increasing the lateral load in vulnerable terrain. Weight of such trees surcharges the slope, increasing normal and downhill force components, and may cause failure during the monsoon (Ghimire 2011). In case of forest plant community, landslides are more associated with the communities of *Fagio-Parrio-Carpinetum betulus* and *Parrio-Carpinetum betulus*. In the study area, these plant communities are strongly correlated with steep and unstable slopes. Although *Parrotia persica* and *Carpinus betulus* have been identified as

Table 2 Frequency ratio values of the landslide-conditioning factors

Conditioning factor	Class	Number of pixels in domain	Number of landslides	% Total of area (*a*)	% Total of landslide area (*b*)	FR (*b*/*a*)
Slope angle	0–5	7,061	3	5.58	4.17	0.75
	5–15	36,700	8	28.98	11.11	0.38
	15–30	53,543	38	42.28	52.78	1.25
	30–50	26,981	23	21.31	31.94	1.50
	>50	2,354	0	1.86	0.00	0.00
Slope aspect	F	180	0	0.14	0.00	0.00
	N	27,135	11	21.43	15.28	0.71
	NE	20,032	1	15.82	1.39	0.09
	E	18,587	19	14.68	26.39	1.80
	SE	19,873	14	15.69	19.44	1.24
	S	12,275	5	9.69	6.94	0.72
	SW	5,024	1	3.97	1.39	0.35
	W	6,982	6	5.51	8.33	1.51
	NW	16,551	15	13.07	20.83	1.59
Altitude (m)	0–600	13,705	33	10.82	45.83	4.24
	600–1,200	43,928	17	34.69	23.61	0.68
	1,200–1,800	65,077	22	51.39	30.56	0.59
	>1,800	3,929	0	3.10	0.00	0.000
Plan curvature (100/m)	Concave	41,880	30	33.07	41.67	1.26
	Flat	31,739	15	25.06	20.83	0.83
	Convex	53,020	27	41.87	37.50	0.90
TWI	<8	22,705	17	17.93	23.61	1.32
	8–12	94,036	41	74.26	56.94	0.77
	>12	9,898	14	7.82	19.44	2.49
SPI	0–150	14,111	3	11.14	4.17	0.37
	150–300	11,124	4	8.78	5.56	0.63
	300–450	9,887	2	7.81	2.78	0.36
	450–600	8,545	7	6.75	9.72	1.44
	>600	82,972	56	65.52	77.78	1.19
STI	0–20	22,876	4	18.06	5.56	0.31
	20–40	22,797	6	18.00	8.33	0.46
	40–60	20,229	10	15.97	13.89	0.87
	60–80	15,605	15	12.32	20.83	1.69
	>80	45,132	37	35.64	51.39	1.44
Lithology	Q^{al}	1,700	0	1.34	0.00	0.00
	K_2^1	10,368	2	8.19	2.78	0.34
	K_1^1	31,849	21	25.15	29.17	1.16
	K_2^{ml}	30,309	20	23.93	27.78	1.16
	R_3^{sh1}	5,479	4	4.33	5.56	1.28
	R_2dl	37,160	16	29.34	22.22	0.76
	P_n	6,582	0	5.20	0.00	0.00
	P_r	3,192	9	2.52	12.50	4.96
Distance to streams (m)	0–100	76,116	54	60.10	75.00	1.25
	100–200	30,738	13	24.27	18.06	0.74
	200–300	9,498	3	7.50	4.17	0.56
	300–400	3,923	1	3.10	1.39	0.45
	>400	6,364	1	5.03	1.39	0.28

Table 2 continued

Conditioning factor	Class	Number of pixels in domain	Number of landslides	% Total of area (*a*)	% Total of landslide area (*b*)	FR (*b*/*a*)
Distance to faults (m)	0–100	15,442	6	12.19	8.33	0.68
	100–200	13,567	13	10.71	18.06	1.69
	200–300	13,266	13	10.48	18.06	1.72
	300–400	11,891	4	9.39	5.56	0.59
	>400	72,473	36	57.23	50.00	0.87
Rainfall (mm)	414–529	9,220	0	7.28	0.00	0.00
	530–645	63,812	23	50.39	31.94	0.63
	646–761	35,427	16	27.97	22.22	0.79
	762–879	18,180	33	14.36	45.83	3.19
NDVI	<0.1	321	0	0.25	0.00	0.00
	0.1–0.3	463	0	0.37	0.00	0.00
	0.3–0.5	11,265	40	8.90	55.56	6.25
	>0.5	114,590	32	90.49	44.44	0.49
Forest canopy (%)	0–40	1,226	1	0.97	1.39	1.43
	40–50	2,864	2	2.26	2.78	1.23
	50–60	5,370	0	4.24	0.00	0.00
	60–70	21,252	20	16.78	27.78	1.66
	70–80	29,185	25	23.05	34.72	1.51
	>80	66,742	24	52.70	33.33	0.63
Timber volume (m^3/ha)	0–100	4,355	3	3.44	4.17	1.21
	100–200	5,309	1	4.19	1.39	0.33
	200–300	22,387	13	17.68	18.06	1.02
	300–400	56,153	41	44.34	56.94	1.28
	400–500	28,252	11	22.31	15.28	0.68
	>500	10,183	3	8.04	4.17	0.52
Plant community	*Fagetum orientalis*	54,858	20	43.32	27.78	0.64
	Fagio-Carpinetum betulus	24,930	12	19.69	16.67	0.85
	Carpino-Quercetum castaneifolia	10,131	2	8.00	2.78	0.35
	Parrio-Carpinetum betulus	9,561	8	7.55	11.11	1.47
	Fagio-Carpino-Quercetum castaneifolia	5,837	1	4.61	1.39	0.30
	Fagio-Parrio-Carpinetum betulus	21,322	29	16.84	40.28	2.39

a potential restoration species for revegetating steep slopes (Abdi et al. 2010), their relatively sparse crown makes them relatively ineffective at insuring slope stability (Sefidi et al. 2011). For timber volume, the results show that the range between 0–100, 200–300, and 300–400 m^3/ha is relatively favorable (highly susceptible) for landslide occurrence. Their frequency ratios are 1.23, 1.02, and 1.28, respectively. With regard to forest canopy, the classes of 50–60 % and >80 % seem to have the lowest impact on landslide occurrence. Their frequency ratios are 0.00 and 0.63, respectively. In forest ecosystems, canopy acts as a shelter and reduces soil erosion and landslide occurrence. The final result of frequency ratio model is a LSI map, in which the LSI values vary from 7.91 to 47.48.

Application of index of entropy model

In landslide susceptibility mapping using frequency ratio model, it was assumed that all the conditioning factors carry equal weight in determining the vulnerability status of the pixels. However, a factor is considered as non-existing and is ignored for the study when it has the same value throughout the study area. According to the Sharma et al. (2010), "if 90 % of the study area has same value and only 10 % of the study area has different values for a particular parameter, the overall role of this parameter in determining the vulnerability status in the study area should be less than any other parameter whose values exhibit consistent and uniform variation throughout the

Table 3 Entropy values of the landslide-conditioning factors

Conditioning factor	Class	*a*	*b*	P_{ij}	(P_{ij})	H_j	$H_{j\ max}$	I_j	W_j
Slope angle	0–5	5.58	4.17	0.747	0.193	1.844	2.322	0.206	0.160
	5–15	28.98	11.11	0.383	0.099				
	15–30	42.28	52.78	1.248	0.322				
	30–50	21.31	31.94	1.499	0.387				
	>50	1.86	0.00	0.000	0.000				
Slope aspect	F	0.14	0.00	0.000	0.000	2.709	3.170	0.145	0.129
	N	21.43	15.28	0.713	0.089				
	NE	15.82	1.39	0.088	0.011				
	E	14.68	26.39	1.798	0.224				
	SE	15.69	19.44	1.239	0.155				
	S	9.69	6.94	0.716	0.089				
	SW	3.97	1.39	0.350	0.044				
	W	5.51	8.33	1.511	0.189				
	NW	13.07	20.83	1.594	0.199				
Altitude (m)	0–600	10.82	45.83	4.235	0.769	1.011	2.000	0.494	0.681
	600–1,200	34.69	23.61	0.681	0.124				
	1,200–1,800	51.39	30.56	0.595	0.108				
	>1,800	3.10	0.00	0.000	0.000				
Plan curvature (100/m)	Concave	33.07	41.67	1.260	0.422	1.560	1.585	0.016	0.016
	Flat	25.06	20.83	0.831	0.278				
	Convex	41.87	37.50	0.896	0.300				
TWI	<8	17.93	23.61	1.317	0.288	1.427	1.585	0.100	0.152
	8–12	74.26	56.94	0.767	0.168				
	>12	7.82	19.44	2.488	0.544				
SPI	0–150	11.14	4.17	0.374	0.094	2.103	2.322	0.094	0.075
	150–300	8.78	5.56	0.632	0.159				
	300–450	7.81	2.78	0.356	0.089				
	450–600	6.75	9.72	1.441	0.361				
	>600	65.52	77.78	1.187	0.298				
STI	0–20	18.06	5.56	0.308	0.064	2.081	2.322	0.104	0.099
	20–40	18.00	8.33	0.463	0.097				
	40–60	15.97	13.89	0.869	0.182				
	60–80	12.32	20.83	1.691	0.354				
	>80	35.64	51.39	1.442	0.302				
Lithology	Q^{al}	1.34	0.00	0.339	0.035	2.073	3.000	0.309	0.373
	K_2^1	8.19	2.78	1.284	0.133				
	K_1^1	25.15	29.17	1.160	0.120				
	K_2^{ml}	23.93	27.78	1.161	0.120				
	R_3^{sh1}	4.33	5.56	0.000	0.000				
	R_2dl	29.34	22.22	0.757	0.078				
	P_n	5.20	0.00	0.000	0.000				
	P_r	2.52	12.50	4.959	0.513				
Distance to streams (m)	0–100	60.10	75.00	1.248	0.381	2.145	2.322	0.076	0.050
	100–200	24.27	18.06	0.744	0.227				
	200–300	7.50	4.17	0.556	0.170				
	300–400	3.10	1.39	0.448	0.137				
	>400	5.03	1.39	0.276	0.084				

Table 3 continued

Conditioning factor	Class	a	b	P_{ij}	(P_{ij})	H_j	$H_{j\ max}$	I_j	W_j
Distance to faults (m)	0–100	12.19	8.33	0.683	0.123	2.181	2.322	0.061	0.067
	100–200	10.71	18.06	1.685	0.303				
	200–300	10.48	18.06	1.724	0.310				
	300–400	9.39	5.56	0.592	0.106				
	>400	57.23	50.00	0.874	0.157				
Rainfall (mm)	414–529	7.28	0.00	0.000	0.000	1.198	2.000	0.401	0.463
	530–645	50.39	31.94	0.634	0.137				
	646–761	27.97	22.22	0.794	0.172				
	762–879	14.36	45.83	3.193	0.691				
NDVI	<0.1	0.25	0.00	0.000	0.000	0.377	2.000	0.812	1.367
	0.1–0.3	0.37	0.00	0.000	0.000				
	0.3–0.5	8.90	55.56	6.245	0.927				
	>0.5	90.49	44.44	0.491	0.073				
Forest canopy (%)	0–40	0.97	1.39	1.435	0.222	2.259	2.585	0.126	0.136
	40–50	2.26	2.78	1.228	0.190				
	50–60	4.24	0.00	0.000	0.000				
	60–70	16.78	27.78	1.655	0.256				
	70–80	23.05	34.72	1.507	0.233				
	>80	52.70	33.33	0.632	0.098				
Timber volume (m^3/ha)	0–100	3.44	4.17	1.212	0.240	2.448	2.585	0.053	0.045
	100–200	4.19	1.39	0.331	0.066				
	200–300	17.68	18.06	1.021	0.202				
	300–400	44.34	56.94	1.284	0.254				
	400–500	22.31	15.28	0.685	0.136				
	>500	8.04	4.17	0.518	0.103				
Plant community	*Fagetum orientalis*	43.32	27.78	0.641	0.107	1.986	2.585	0.232	0.232
	Fagio-Carpinetum betulus	19.69	16.67	0.847	0.141				
	Carpino-Quercetum castaneifolia	8.00	2.78	0.347	0.058				
	Parrio-Carpinetum betulus	7.55	11.11	1.472	0.245				
	Fagio-Carpino-Quercetum castaneifolia	4.61	1.39	0.301	0.050				
	Fagio-Parrio-Carpinetum betulus	16.84	40.28	2.392	0.399				

study area." In this study, we employed index of entropy to reduce the unevenness among the parameters and thereby to provide realistic status of their impact on the landslide susceptibility within the study area. The results show that each class of the conditioning factors is characterized by a certain landslide occurrence density P_{ij} (Eq. 7 and Table 3). Overall, the most important factors controlling the distribution of landslides were derived and are presented in Table 3. The findings based on entropy approach show that NDVI, altitude, and rainfall are the most important factors which explain better the landslide occurrence and distribution in study area. The final landslide susceptibility map was developed using the Eq. (13) as follow:

$$Y_{IOE} = \left(\begin{array}{l} (\text{slope degree} \times 0.16) + (\text{slope aspect} \times 0.129) + (\text{altitude} \times 0.681) + (\text{plan curvature} \times 0.016) \\ + (\text{TWI} \times 0.152) + (\text{SPI} \times 0.075) + (\text{STI} \times 0.099) + (\text{lithology} \times 0.373) + (\text{distance to streams} \times 0.05) \\ + (\text{distance to faults} \times 0.067) + (\text{rainfall} \times 0.463) + (\text{NDVI} \times 1.367) + (\text{forest canopy} \times 0.136) \\ + (\text{timber volume} \times 0.045) + (\text{forest plant community} \times 0.232) \end{array} \right).$$

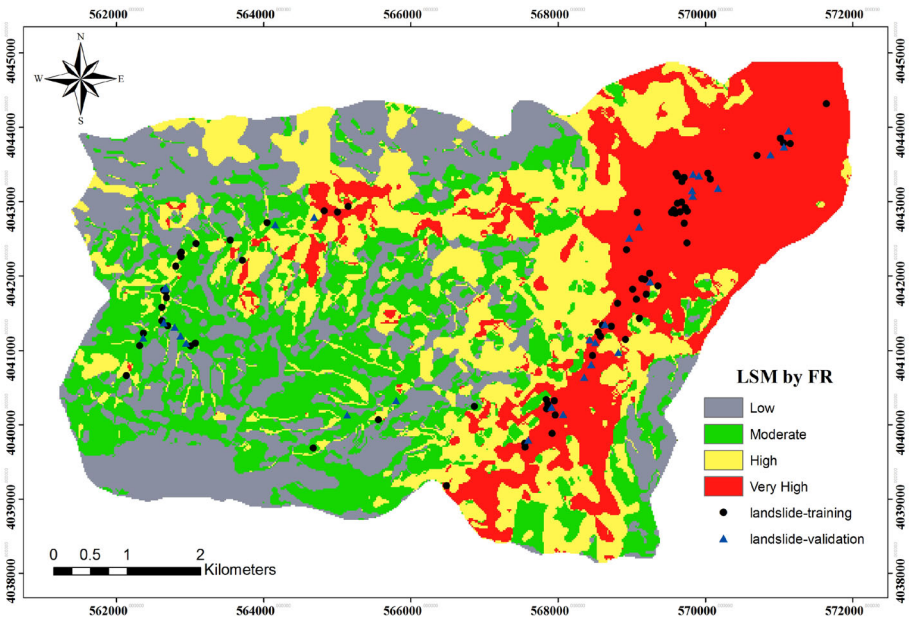

Fig. 7 Landslide susceptibility map produced by frequency ratio model

The final result of index of entropy model is a LSI map, in which the LSI values vary from 1.5965 to 24.5357.

Landslide susceptibility maps

For visual interpretation of LSI maps, the data need to be classified into categorical susceptibility classes. There are many classification methods available, such as quantiles, natural breaks, equal intervals, and standard deviations (Ayalew and Yamagishi 2005). Generally, the selection of classification methods depends on the distribution of the landslide susceptibility indexes (Ayalew and Yamagishi 2005). For instance, if the data distribution is close to normal, equal interval, or standard deviation, classifiers should be used. If the data distribution has a positive or negative skewness, the quantile or natural break distribution classifiers could be chosen (Akgun et al. 2012). In this study, considering data distribution histogram, the quantile and natural break classifiers were applied to the data. The comparison results indicated that the quantile classifier was able to produce better results than the natural break classifier. Therefore, the quantile data classification approach was chosen, and the landslide susceptibility index maps were classified into four susceptibility classes: low, moderate, high, and very high (Pourghasemi et al. 2012b). According to the landslide susceptibility map generated with the frequency ratio model (Fig. 7), 24.49 % of the total area falls in the low susceptibility zone. Moderate and high susceptible zones represent 26.06 and 24.93 % of the total area, respectively. The very high landslide susceptibility zone includes 24.52 % of the total study area. In landslide susceptibility map produced from index of entropy model (Fig. 8), the low susceptible zone covers 22.84 % of the total study area, whereas moderate, high, and very high susceptible zone cover 26.77, 26.76, and 23.63 % of the total area, respectively.

Validation of the landslide susceptibility maps

Any effort to make certain landslide susceptibility in a region needs proper validation. Confirmation should establish the quality (i.e., consistency, robustness, degree of fitting, and prediction skill) of the proposed susceptibility estimate (Yalcin et al. 2011). In our study, validation of the susceptibility maps was checked by receiver operating characteristics (ROC) (Akgun et al. 2012; Bui et al. 2012; Ozdemir and Altural 2013). The ROC curve is a useful method for representing the quality of deterministic and probabilistic detection and forecast systems. The ROC plots the different accuracy values obtained against the whole range of possible threshold values of the functions, and the ROC serves as a global accuracy statistic for the model, regardless of a specific discriminate threshold (Pourghasemi et al. 2012c). In the ROC curve, the sensitivity of the model (in our case, the percentage of unstable pixels correctly predicted by the model) is plotted against 1-specificity (the percentage of predicted unstable pixels over the total) (Mohammady et al. 2012). The area under the ROC curve (AUC) characterizes the quality of the probabilistic model by describing its ability to reliably predict an occurrence or non-occurrence event. The range of values of the AUC is 0.5–1 for a good fit, while values below 0.5 represent a random fit. For validation, we used both success rate and prediction rate curves by comparing the existing landslide locations with the landslide susceptibility maps. The success rate results were obtained by using the training dataset 70 % (72 landslide locations).

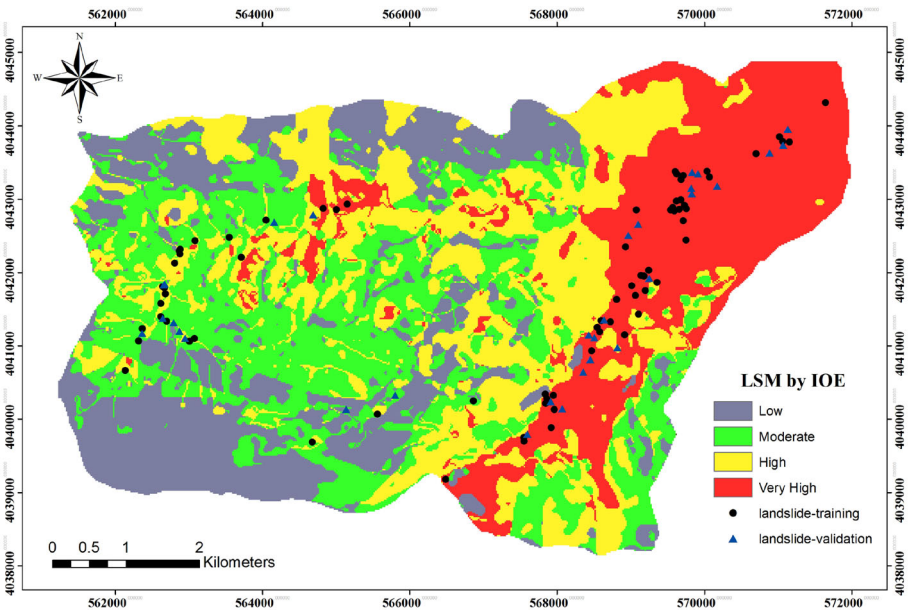

Fig. 8 Landslide susceptibility map produced by index of entropy model

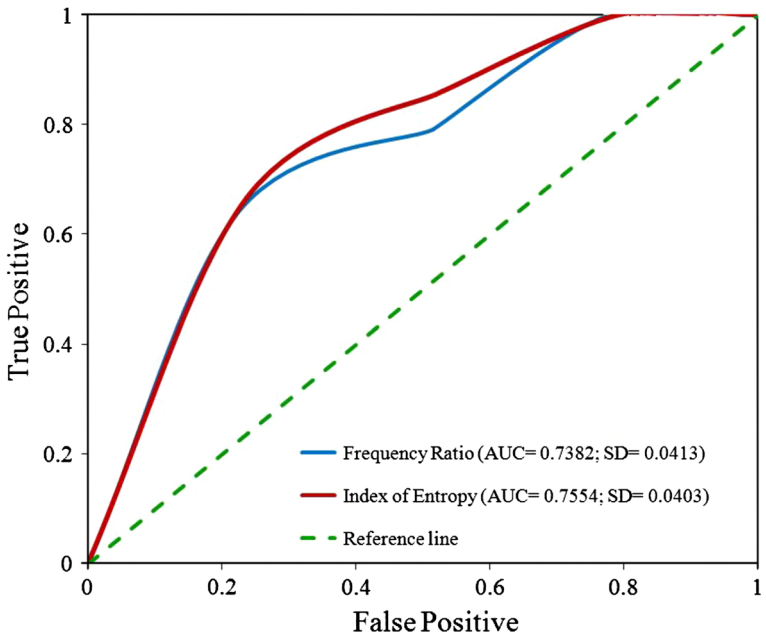

Fig. 9 Success rate curves for the susceptibility maps produced in this study

Figure 9 shows the success rate curve for landslide susceptibility maps, which were classified by quantile data classification approach. The index of entropy model has the highest AUC value (0.7554), whereas frequency ratio has 0.7382. Since the success rate method used the training landslide pixels that have already been used for building the landslide models, the success rate is not a suitable method for assessing the prediction capability of the models. However, the success rate method may help to determine how well the resulting landslide susceptibility maps have classified the areas of existing landslides (Bui et al. 2012; Pourghasemi et al. 2012c).

The prediction rate explains how well the model and predictor variable predict the landslide. This method is already widely used as a measure of performance of a predictive rule (e.g., Mohammady et al. 2012; Akgun et al. 2012; Ozdemir and Altural 2013). In our study, the AUC values of the prediction rate curves for frequency ratio and index of entropy models were found to be 0.7268, and 0.7559, respectively. It can be concluded that both the success rate and prediction rate curve show almost similar result, and the models utilized in this study showed reasonably good accuracy in predicting the landslide susceptibility of the study area (Fig. 10).

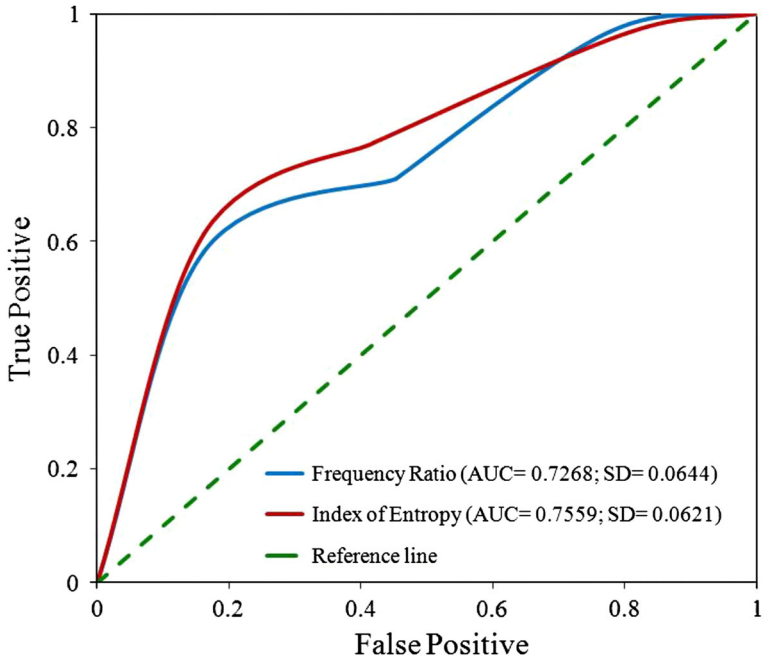

Fig. 10 Prediction rate curves for the susceptibility maps produced in this study

As already mentioned, the natural break classifier was also used to classify the LSI maps into categorical susceptibility classes. Furthermore, the obtained maps were validated by ROC method. In the case of success rate, the frequency ratio and index of entropy models showed the AUC values of 0.7242, and 0.7195, respectively. For prediction accuracy, the AUC values were 0.6977, and 0.6833, respectively. The comparison results indicate that the quantile classifier performs better than the natural break in classification LSI maps produced in this study.

Conclusion

Landslides are the most frequent natural hazards in the Caspian forest. However, progress in susceptibility mapping at the operational scale lags behind. This study applied widely accepted models, frequency ratio, and index of entropy, within a GIS environment for the purpose of LSM. Although previous studies have applied these models to produce LS maps, the efficiency and effectiveness of which had not been evaluated in forestlands before the present study. The ROC plots showed that the accuracy of the LS maps produced by the frequency ratio and index of entropy models was 72.68 and 75.59 %, respectively. Furthermore, we have found the models relatively flexible and easy to use. While complex models provide a basis for building and consolidating scientific knowledge, simple models are more useful and easily applied for land management purposes. One should always keep in mind that ''simple is the best'' in engineering applications. LSM using GIS-based frequency ratio and index of entropy models has the advantages of (1) allowing catchment-scale assessment, (2) incorporating a wide range of the factors thought to affect occurrence of landslide phenomena, and (3) discriminating the considered factors to help the managers to understand which factors are the most important to trigger landslide phenomena.

The landslide susceptibility maps produced in this study can provide a cheap and comprehensive assessment of the study area for its capacity for supporting individual uses or combination of uses, such as road construction and timber harvesting. Managers and foresters can then make decisions and prepare prescriptions that will have highly predictable results for producing sustainable products, maintaining site quality, and substantially reducing risk of any adverse impacts.

Acknowledgments This work was supported by the Tarbiat Modares University. Abdullah Abbasi, Sattar Ezzati, Hamed Asadi, and Mostafa Adib are thanked for their assistance in field surveys. The authors also express their sincere appreciation to the anonymous reviewers for their helpful and valuable detailed comments and suggestions.

References

Abdi E, Majnounian B, Genet M, Rahimi H (2010) Quantifying the effects of root reinforcement of Persian Ironwood (*Parrotia persica*) on slope stability; a case study: Hillslope of Hyrcanian forests, northern Iran. Ecol Eng 36(10):1409–1416

Akgun A, Sezer EA, Nefesliogl HA, Gokceoglu C, Pradhan B (2012) An easy-to-use MATLAB program (MamLand) for the assessment of landslide susceptibility using a Mamdani fuzzy algorithm. Comput Geosci 38:23–34

Ayalew L, Yamagishi H (2004) Slope movements in the Blue Nile basin, as seen from landscape evolution perspective. Geomorphology 57:95–116

Ayalew L, Yamagishi H (2005) The application of GIS-based logistic regression for landslide susceptibility mapping in the Kakuda–Yahiko Mountains, Central Japan. Geomorphology 65(1–2): 15–31

Bagnold RA (1966) An Approach to the Sediment Transport Problem from General Physics. USGS Professional Paper, Washington, DC

Bednarik M, Magulová B, Matys M, Marschalko M (2010) Landslide susceptibility assessment of the Kraľovany–Liptovský Mikuláš railway case study. Phys Chem Earth Parts A/B/C 35(3):162–171

Bednarik M, Yilmaz I, Marschalko M (2012) Landslide hazard and risk assessment: a case study from the Hlohovec–Sered'landslide area in south-west Slovakia. Nat Hazards 64(1):547–575

Bell FG (1998) Environmental geology: principles and practice. Wiley-Blackwell, NY

Beven KJ, Kirkby MJ (1979) A physically-based variable contributing area model of basin hydrology. Hydrol Sci Bull 24:43–69

Bui TD, Pradhan B, Lofman O, Revhaug I, Dick OB (2012) Spatial prediction of landslide hazards in Hoa Binh province (Vietnam): a comparative assessment of the efficacy of evidential belief functions and fuzzy logic models. Catena 96:28–40

Constantin M, Bednarik M, Jurchescu MC, Vlaicu M (2011) Landslide susceptibility assessment using the bivariate statistical analysis and the index of entropy in the Sibiciu Basin (Romania). Environ Earth Sci 63:397–406

Dai FC, Lee CF, Xu ZW (2001) Assessment of landslide susceptibility on the natural terrain of Lantau Island, Hong Kong. Environ Geol 40(3):381–391

Das I, Stein A, Kerle N, Dadhwal VK (2012) Landslide susceptibility mapping along road corridors in the Indian Himalayas using Bayesian logistic regression models. Geomorphology 179: 116–125

Devkota KC, Regmi AD, Pourghasemi HR, Yoshida K, Pradhan B, Ryu IC, Dhital MR, Althuwaynee OF (2013) Landslide susceptibility mapping using certainty factor, index of entropy and logistic regression models in GIS and their comparison at Mugling–Narayanghat road section in Nepal Himalaya. Nat Hazards 65:1–31

Didham RK, Fagan LL (2004) Forest Canopies. Encyclopedia of forest science. Elsevier, Amsterdam, pp 68–80

Ercanoglu M, Gokceoglu C (2002) Assessment of landslide susceptibility for a landslide-prone area (North of Yenice, NW Turkey) by fuzzy approach. Environ Geol 41:720–730

Feizizadeh B, Blaschke T (2013) GIS-multicriteria decision analysis for landslide susceptibility mapping: comparing three methods for the Urmia lake basin, Iran. Nat Hazards 65:2105–2128

Fernandes NF, Guimaraes RF, Gomes RAT, Vieira BC, Montgomery DR, Greenberg H (2004) Topographic controls of landslides in Rio de Janeiro: field evidence and modelling. Catena 55:163–181

Ghajar I, Najafi A, Torabi SA, Khamehchiyan M, Boston K (2012) An adaptive network-based fuzzy inference system for rock share estimation in forest road construction. Croat J For Eng 33(2):313–328

Ghimire M (2011) Landslide occurrence and its relation with terrain factors in the Siwalik Hills, Nepal: case study of susceptibility assessment in three basins. Nat Hazards 56(1):299–320

Gokceoglu C, Sonmez H, Nefeslioglu HA, Duman TY, Can T (2005) The 17 March 2005 Kuzulu landslide (Sivas, Turkey) and landslide-susceptibility map of its near vicinity. Eng Geol 81:65–83

Guzzetti F, Carrara A, Cardinali M, Reichenbach P (1999) Landslide hazard evaluation: a review of current techniques and their application in a multi-scale study, Central Italy. Geomorphology 31:181–216

Hall FG, Towhshend JR, Engman ET (1995) Status of remote sensing algorithms for estimation of land surface state parameters. Rem Sens Environ 51:138–156

Iranian Plan and Budget Organization (IPBO) (2000) Guidelines for design, execute and using forest roads No: 131, 2nd edn. Office of the Deputy for Technical Affairs. Bureau of Technical Affairs and Standards, 170 pp

Kamp U, Growley BJ, Khattak GA, Owen LA (2008) GIS-based landslide susceptibility mapping for the 2005 Kashmir earthquake region. Geomorphology 101(4):631–642

Khanh NQ (2009) Landslide hazard assessment in muonglay, Vietnam applying GIS and remote sensing. Dr.rer. nat. at the Faculty of Mathematics and Natural Sciences Ernst-Moritz-Arndt- University Greifswald. http://deposit.ddb.de/cgibin/dokserv?idn=1009125575&dok_var=d1&dok_ext=pdf&filename=1009125575.pdf

Larsen MC, Parks JE (1997) How wide is a road? The association of roads and mass-wasting in a forested mountain environment. Earth Surf Proc Land 22:835–848

Lee S, Pradhan B (2007) Landslide hazard mapping at Selangor, Malaysia using frequency ratio and logistic regression models. Landslides 4:33–41

Mohammady M, Pourghasemi HR, Pradhan B (2012) Landslide susceptibility mapping at Golestan Province Iran: a comparison between frequency ratio, Dempster-Shafer, and weights-of evidence models. J Asian Earth Sci 61:221–236

Moore ID, Burch GJ (1986) Physical basis of the length-slope factor in the Universal Soil Loss Equation. Soil Sci Soc Am J 50(5):1294–1298

Moore ID, Grayson RB, Ladson AR (1991) Digital terrain modeling: a review of hydrological, geomorphological, and biological applications. Hydrol Process 5:3–30

Oh HJ, Pradhan B (2011) Application of a neuro-fuzzy model to landslide susceptibility mapping for shallow landslides in a tropical hilly area. Comput Geosci 37:1264–1276

Ozdemir A, Altural T (2013) A comparative study of frequency ratio, weights of evidence and logistic regression methods for landslide susceptibility mapping: Sultan Mountains, SW Turkey. J Asian Earth Sci 64:180–197

Pachauri AK, Pant M (1992) Landslide hazard mapping based on geological attributes. Eng Geol 32:81–100

Papathanassiou G, Valkaniotis S, Ganas A, Pavlides S (2012) GIS-based statistical analysis of the spatial distribution of earthquake-induced landslides in the island of Lefkada, Ionian Islands, Greece. Landslides. doi:10.1007/s10346-012-0357-1

Pourghasemi HR, Gokceoglu C, Pradhan B, Deylami Moezzi K (2012a) Landslide susceptibility mapping using a spatial multi criteria evaluation model: case study at Haraz Watershed, Iran. In: Pradhan B, Buchroithner M (eds) Terrigenous Mass Movements. Springer, Berlin, pp 23–49

Pourghasemi HR, Mohammady M, Pradhan B (2012b) Landslide susceptibility mapping using index of entropy and conditional probability models in GIS: Safarood Basin, Iran. Catena 97:71–84

Pourghasemi HR, Pradhan B, Gokceoglu C (2012c) Application of fuzzy logic and analytical hierarchy process (AHP) to landslide susceptibility mapping at Haraz watershed, Iran. Nat Hazards 63(2):965–996

Pourghasemi HR, Moradi HR, Fatemi Aghda SM, Gokceoglu C, Pradhan B (2013) GIS-based landslide susceptibility mapping with probabilistic likelihood ratio and spatial multi-criteria evaluation models (North of Tehran, Iran). Arab J Geosci. doi:10.1007/s12517-012-0825-x

Pradhan B (2013) A comparative study on the predictive ability of the decision tree, support vector machine and neuro-fuzzy models in

landslide susceptibility mapping using GIS. Comput Geosci 51:350–365

Regmi AD, Devkota KC, Yoshida K, Pradhan B, Pourghasemi HR, Kumamoto T, Akgun A (2013) Application of frequency ratio, statistical index, and weights-of-evidence models and their comparison in landslide susceptibility mapping in Central Nepal Himalaya. Arab J Geosci. doi:10.1007/s12517-012-0807-z

Sefidi K, Marvie Mohadjer MR, Etemad V, Copenheaver CA (2011) Stand characteristics and distribution of a relict population of Persian ironwood (*Parrotia persica* Meyer) in northern Iran. Flora 206(5):418–422

Sharma LP, Nilanchal P, Ghose MK, Debnath P (2010) Influence of Shannon's entropy on landslide-causing parameters for vulnerability study and zonation—a case study in Sikkim, India. Arab J Geosci 5(3):421–431

Vorpahl P, Elsenbeer H, Märker M, Schröder B (2012) How can statistical models help to determine driving factors of landslides? Ecol Model 239:27–39

Yalcin A, Reis S, Aydinoglu AC, Yomralioglu T (2011) A GIS-based comparative study of frequency ratio, analytical hierarchy process, bivariate statistics and logistics regression methods for landslide susceptibility mapping in Trabzon, NE Turkey. Catena 85(3):274–287

Yilmaz I (2009) Landslide susceptibility mapping using frequency ratio, logistic regression, artificial neural networks and their comparison: a case study from Kat landslides (Tokat-Turkey). Comput Geosci 35:1125–1138

Yilmaz I, Keskin I (2009) GIS based statistical and physical approaches to landslide susceptibility mapping (Sebinkarahisar, Turkey). Bull Eng Geol Environ 68:459–471

Yufeng S, Fengxiang J (2009) Landslide stability analysis based on generalized information entropy. Int Conf Environ Sci Inf Appl Technol 2:83–85